

Fully automated structure determinations of the Fes SH2 domain using different sets of NMR spectra

Anna Scott, Blanca López-Méndez and Peter Güntert*

Tatsuo Miyazawa Memorial Program, RIKEN Genomic Sciences Center, 1-7-22 Suehiro, Tsurumi, Yokohama 230-0045, Japan

Received 13 December 2005; Revised 17 February 2006; Accepted 28 February 2006

The recently introduced fully automated protein NMR structure determination algorithm (FLYA) yields, without any human intervention, a three-dimensional (3D) protein structure starting from a set of two- and three-dimensional NMR spectra. This paper investigates the influence of reduced sets of experimental spectra on the quality of NMR structures obtained with FLYA. In a case study using the Src homology domain 2 from the human feline sarcoma oncogene Fes (Fes SH2), five reduced data sets selected from the full set of 13 three-dimensional spectra of the previously determined conventional structure were used to calculate the protein structure. Three reduced data sets utilized only CBCA(CO)NH and CBCANH for the backbone assignments and two data sets used only CBCA(CO)NH. All, some, or none of the five original side-chain assignment spectra were used. Results were compared with those of a FLYA calculation for the complete set of spectra and those of the conventionally determined structure. In four of the five cases tested, the three-dimensional structures deviated by less than 1.3 Å in backbone RMSD from the conventionally determined Fes SH2 reference structure, showing that the FLYA algorithm is remarkably stable and accurate when used with reduced sets of input spectra. Copyright © 2006 John Wiley & Sons, Ltd.

KEYWORDS: NMR; ^1H ; ^{15}N ; ^{13}C ; Fes SH2; protein structure; automated assignment; CYANA; FLYA

INTRODUCTION

Until recently it was not possible to determine an NMR protein structure without manual analysis of the data and chemical shift assignments, although many computational approaches have been introduced either to support the interactive analysis by visualization and book-keeping, or to provide automation for specific parts of an NMR structure determination.^{1–4} Automated procedures are now widely accepted, e.g. for the assignment of NOE distance restraints and the structure calculations.^{3–7} Present systems designed to handle the whole NMR structure determination process, however, generally require certain human interventions.^{3,7} The recently introduced fully automated protein NMR structure determination algorithm (FLYA) is a significant advancement because it can solve NMR protein structures by purely computational means using only the primary structure and processed NMR spectra as the input. (López-Méndez B, Güntert P. *J. Am. Chem. Soc.* Submitted) The FLYA algorithm can decrease significantly the time required to determine a protein structure. This is particularly valuable for NMR-based structural genomics initiatives where a large number of structures need to be solved as quickly and efficiently as possible. Depending on the characteristics of the protein whose structure is being solved, different

NMR spectra can be used for structure determination. FLYA has been tested successfully for three 12–16 kDa proteins, including the Src homology domain 2 from the human feline sarcoma oncogene Fes (Fes SH2).⁸ Because there is no unique standard set of experiments for structure determination, it is desirable to understand the limitations of the FLYA algorithm when used with a reduced number of NMR spectra. Additionally, being able to calculate good quality structures with a minimum number of experiments would be advantageous to researchers. The Fes SH2 domain structure (PDB code 1WQU) was originally solved by manual chemical shift assignment and automated NOE assignment with the program CYANA.^{8,9} Here we use the NMR spectra available from the conventional structure determination of the Fes SH2 protein to calculate protein structures on the basis of reduced numbers of experiments.

EXPERIMENTAL

Computational methods

The FLYA algorithm was used to generate the Fes SH2 protein structures. This method will be described in detail elsewhere. (López-Méndez B, Güntert P. *J. Am. Chem. Soc.* Submitted) In brief, the algorithm uses as input data only the protein sequence and multidimensional NMR spectra. Peaks are identified in the multidimensional NMR spectra using the automated peak picking algorithm of NMRView,¹⁰ and the peak lists are prepared by CYANA.^{4,11} Depending on the spectra, the preparation included unfolding aliased

*Correspondence to: Peter Güntert, RIKEN Genomic Sciences Center, 1-7-22 Suehiro, Tsurumi, Yokohama 230-0045, Japan.
E-mail: guentert@gsc.riken.jp

signals, systematic correction of chemical shift referencing, and removal of peaks near the diagonal or water lines. The peak lists resulting from this step remained invariable throughout the rest of the procedure. An ensemble of initial chemical shift assignments was obtained by multiple runs of a modified version of the GARANT algorithm^{12,13} with different seed values for the random number generator.¹⁴ The peak position tolerance was set to 0.03 ppm for the ¹H dimensions and to 0.4 ppm for the ¹³C and ¹⁵N dimensions. These initial chemical shift assignments were consolidated by CYANA into a single consensus chemical shift list. The consensus chemical shift list, the amino acid sequence, and the unassigned NOE peak lists were used as input data for combined automated NOE assignment⁶ and structure calculation¹¹ using a new version of the software CYANA. Seven cycles of combined automated NOE assignment and structure calculation by simulated annealing in torsion angle space, and a final structure calculation using only the unambiguously assigned distance restraints were run. The complete calculation comprised three stages. In the first stage, the chemical shifts and protein structures were generated *de novo* (stage I). In the next stages (stages II and III), the structures generated in the preceding stage were used as additional input for the determination of chemical shift assignments. Stages II and III are particularly important for aromatic residues and other resonances whose assignments rely on through-space NOESY information. At the end of the third stage, the 20 final CYANA conformers with the lowest target function values were subjected to restrained energy minimization in explicit solvent against the AMBER force field¹⁵ using the program OPALp.^{16,17} The complete procedure was driven by the NMR structure calculation program CYANA,^{4,11} which was also used for parallelization of all the time-consuming steps. Calculations were performed simultaneously on 20 processors of a Linux cluster system with Intel Xeon 3.06 GHz processors and 2 GB of memory per 2-processor node, and required about 30 h of computation time for a complete FLYA run. Three runs were conducted with each set of NMR spectra using different seed values for the random number generators. The results of these three runs were averaged and are presented in the Section on Results and Discussion.

Protein

The FLYA algorithm was applied to determine the structure of the Src homology domain 2 from the human feline sarcoma oncogene Fes (Fes SH2), whose resonance assignments⁹ and high-quality NMR solution structure⁸ were previously determined using conventional techniques. Fes SH2 comprises 114 residues and has the canonical Src homology 2 domain fold with a central three-stranded antiparallel β -sheet flanked on either side by an α -helix, and three short antiparallel β -strands that pack against the second α -helix.⁸ The seven N-terminal and six C-terminal residues are non-native flanking regions related to the expression and purification system and are disordered in solution⁸ so that the structured region of the protein is residues 8–108. The Fes SH2 coordinates and chemical shift assignments determined earlier by conventional methods are available from the Protein Data Bank

with accession code 1WQU and from the BioMagResBank with accession number 6331.

NMR spectroscopy and spectral processing

The NMR measurements recorded for the previous conventional structure determination were also used for this study. They were collected at 25 °C on a Bruker DRX 600 spectrometer operating at a proton frequency of 600 MHz and using an *xyz*-gradient triple-resonance probe, with the exception of the NOESY spectra that were recorded on a Bruker AV 800 spectrometer operating at a proton frequency of 800 MHz and equipped with a triple-resonance ^1H , ^{13}C , ^{15}N probe with triple-axis pulse field gradients. Table 1 gives a summary of the spectra acquired, and the [^1H , ^{15}N]-HSQC spectrum in Fig. 1 illustrates the quality of the NMR data for Fes SH2. Further details about the NMR experiments are given in Refs 8, 9. The NMR measurements were carried out with one uniformly ^{13}C - and ^{15}N -labeled sample containing 1.2 mM protein dissolved in 90% H_2O /10% D_2O (v/v), 20 mM Tris-HCl buffer, pH 7.0, 100 mM NaCl, 1 mM dithiothreitol, and 0.02% NaN_3 .⁹ The program NMRPipe¹⁸ was used for spectral processing. At least twofold zero-filling in each spectral dimension, linear prediction in one indirect dimension, apodization by 60–90° shifted sine-squared window functions, and baseline correction along all dimensions were applied. Whenever possible, the same parameters were used for processing the corresponding dimensions of all experiments. Particular attention was paid to accurate and consistent chemical shift referencing in the direct and indirect dimensions to enable the use of small tolerances for the matching of peak positions from different spectra during the fully automated analysis.

Analysis and structure comparison

The program MOLMOL¹⁹ was used to visualize three-dimensional (3D) structures. CYANA was used to obtain statistics on target function values, restraint violations, etc. RMSD values to the mean coordinates of a structure bundle for superpositions of the backbone atoms N, C^α and C' or the heavy atoms in the structured region of residues 8–108 were calculated with CYANA. The single RMSD

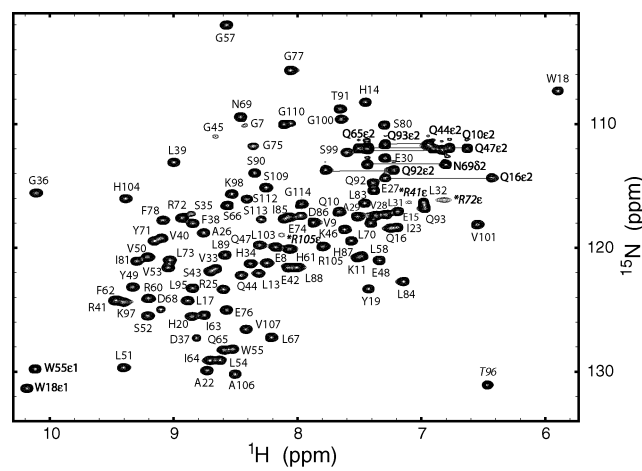


Figure 1. $[^1\text{H}, ^{15}\text{N}]$ -HSQC spectrum of the Fes SH2 domain. Folded peaks are labeled with asterisks.

Table 1. Acquisition parameters for the multidimensional NMR spectra recorded for Fes SH2 and a summary of spectra used for the FLYA runs 1 to 6

Spectrum	Nuclei ^a	Points ^b	Spectral width ^c (kHz)	Spectra used in FLYA run					
				1	2	3	4	5	6
2D spectra	–	–	–	2	2	2	2	2	2
¹⁵ N-HSQC	¹⁵ N	46	11.2, 2.7	Yes	Yes	Yes	Yes	Yes	Yes
¹³ C-HSQC	¹³ C	40	11.2, 7.9	Yes	Yes	Yes	Yes	Yes	Yes
3D spectra	–	–	–	13	9	8	7	5	3
For backbone assignment									
HNCO	¹⁵ N, ¹³ C	46 × 50	8.4, 2.0, 3.3	Yes	–	–	–	–	–
HN(CA)CO	¹⁵ N, ¹³ C	46 × 50	8.4, 2.0, 3.3	Yes	–	–	–	–	–
HNCA	¹⁵ N, ¹³ C	46 × 50	8.4, 2.0, 4.8	Yes	–	–	–	–	–
HN(CO)CA	¹⁵ N, ¹³ C	46 × 50	8.4, 2.0, 4.8	Yes	–	–	–	–	–
CBCANH	¹⁵ N, ¹³ C	46 × 64	8.4, 2.0, 11.3	Yes	Yes	Yes	Yes	–	–
CBCA(CO)NH	¹⁵ N, ¹³ C	46 × 64	8.4, 2.0, 11.3	Yes	Yes	Yes	Yes	Yes	Yes
For side-chain assignment									
HBHA(CO)NH	¹⁵ N, ¹ H	46 × 64	8.4, 2.0, 8.4	Yes	Yes	Yes	Yes	–	–
(H)CC(CO)NH	¹⁵ N, ¹³ C	46 × 64	8.4, 2.0, 11.3	Yes	Yes	Yes	Yes	Yes	–
H(CCCO)NH	¹⁵ N, ¹ H	46 × 64	8.4, 2.0, 6.7	Yes	Yes	Yes	Yes	Yes	–
HCCH-COSY	¹³ C, ¹ H	50 × 100	8.4, 11.3, 8.4	Yes	Yes	–	–	–	–
HCCH-TOCSY	¹³ C, ¹ H	64 × 100	8.4, 11.3, 8.4	Yes	Yes	Yes	–	–	–
For restraint collection									
¹⁵ N-edited NOESY	¹⁵ N, ¹ H	46 × 128	11.2, 2.7, 11.2	Yes	Yes	Yes	Yes	Yes	Yes
¹³ C-edited NOESY	¹³ C, ¹ H	40 × 150	11.2, 8.0, 11.2	Yes	Yes	Yes	Yes	Yes	Yes

^a Nuclei: nuclei observed in the indirect dimension(s).^b Points: complex time domain data points in the indirect dimensions. For all the spectra, 512 complex time domain data points were recorded in the directly detected ¹H dimension.^c Spectral width: spectral widths in the direct and indirect dimension(s).

value between the two sets of mean coordinates was used to quantify the deviation of one structure bundle from another. Conformational energies were calculated with OPALp^{16,17} using the AMBER¹⁵ force field.

RESULTS AND DISCUSSION

A summary of the NMR spectra collected, and their acquisition parameters are given in Table 1 along with the experiments included in the reduced data sets. For Run 1, the full set of 2 two-dimensional (2D) and thirteen 3D spectra was employed. Runs 2–6 used progressively reduced sets of spectra for the backbone and side-chain chemical shift assignments. The 2D HSQC (Fig. 1) and the 3D NOESY spectra were used in all the runs. Run 2 used nine 3D spectra including all available side-chain experiments and the backbone experiments CBCANH and CBCA(CO)NH. Runs 3 and 4 used the same backbone and side-chain experiments as Run 2 except that they also excluded the HCCH-COSY and HCCH-COSY/HCCH-TOCSY experiments and utilized eight and seven 3D spectra, respectively. Run 5 further omitted the backbone experiment CBCANH and the side-chain experiment HBHA(CO)NH. In the most extreme case, Run 6, a single backbone experiment CBCA(CO)NH was kept besides the NOESY spectra. Automated peak picking yielded peak lists that contained on average about 1.5 times as many entries as would be expected under ideal conditions. Peak picking was always performed over the complete spectrum,

excluding only two narrow bands along the water line and along the diagonal. No other spectral regions or individual peaks were interactively excluded from peak picking.

Table 2 summarizes the chemical shift assignments and provides structural statistics for Runs 1–6. The chemical shift assignments for the structured region of the protein, residues 8–108, were classified into three categories. The first category, 'all', includes all assignable ¹H, ¹³C and, ¹⁵N atoms. The second category, 'backbone, β CH/CH₂', includes only the ¹H, ¹³C, and ¹⁵N atoms in the protein backbone along with the H^β and C^β atoms. The final category, 'other CH_n', includes all the remaining aliphatic and aromatic side-chain assignments except H^β and C^β. Run 1 made use of the HNCO and HN(CA)CO experiments for the assignment of the carbonyl carbons so that the number of assigned nuclei was higher than for Runs 2–6, which did not include the experiments to assign the C' chemical shifts.

Table 2 summarizes for each of the three categories of nuclei the percentage of assignments that are, within a given tolerance, identical to those made by conventional assignment ('equal'), that differ by more than the tolerance from the conventional assignment ('different'), and that do not agree within the tolerance with the conventional assignment of any atom of the same residue ('wrong'). Only the latter type of assignment error can potentially lead to a serious distortion of the resulting structure. For the same reason, ¹³C and ¹⁵N atoms not bound to ¹H

Table 2. Statistics of the Fes SH2 chemical shift assignments and structures determined using the FLYA algorithm and different sets of experimental NMR spectra

Quantity	FLYA run					
	1	2	3	4	5	6
All chemical shift assignments ^{a,b}						
Assigned ^1H , ^{13}C , ^{15}N nuclei	1199	1091	1091	1091	1091	1091
Equal (%)	90	89	88	84	84	77
Different (%)	9	11	11	15	16	23
Wrong (%)	3	4	3	6	7	15
Backbone and βCH_n chemical shift assignments ^{a,b}						
Assigned ^1H , ^{13}C , ^{15}N nuclei	760	659	659	659	659	659
Equal (%)	97	96	96	93	92	88
Different (%)	3	4	3	6	8	14
Wrong (%)	2	2	2	3	6	12
Other CH_n chemical shift assignments ^{a,b}						
Assigned ^1H , ^{13}C , ^{15}N nuclei	439	432	432	432	432	432
Equal (%)	77	78	77	69	71	63
Different (%)	20	21	22	30	28	36
Wrong (%)	5	6	5	11	10	19
Structural statistics						
Assigned NOESY cross peaks	4882	4859	4874	4757	4712	4524
Long-range ($ i - j \geq 5$) distance restraints	1206	1230	1219	1188	1153	1102
Maximal distance restraint violation (Å)	0.15	0.17	0.15	0.15	0.19	0.20
CYANA target function (Å ²)	4.5	3.2	4.4	4.7	7.6	8.8
AMBER energy (kcal/mol)	-3957	-3916	-3948	-3917	-3741	-3663
Backbone RMSD to mean (Å) ^b	0.34	0.30	0.31	0.33	0.35	0.35
All heavy atom RMSD to mean (Å) ^b	0.74	0.71	0.68	0.74	0.72	0.73
Backbone RMSD to reference (Å) ^b	0.97	0.85	1.00	1.06	1.28	2.87
All heavy atom RMSD to reference (Å) ^b	1.37	1.33	1.56	1.56	1.83	3.41

^a Chemical shift assignments are classified as 'equal' when they coincided, within tolerances 0.03 ppm for ^1H and 0.4 ppm for ^{13}C / ^{15}N , with the corresponding shift from the conventional assignment, as 'different' when they differed by more than the tolerance from the value from the conventional assignment, and as 'wrong' when they did not match any conventionally assigned shift within the same residue.

^b For the structured region of residues 8–108.

were excluded when counting the wrong assignments. For chemical shift matching, tolerance values of 0.03 ppm for ^1H and 0.4 ppm for ^{13}C were used throughout. These relatively large tolerances were used in consideration of the moderate precision of the peak positions that can be achieved by automated peak picking. Note that the percentages of equal and different peaks do not necessarily sum up to 100% because only the shifts of nuclei that were assigned simultaneously by both methods could be compared.

As expected, when fewer experiments are used, the number of equal assignments decreases and the number of different and wrong assignments increases. Nevertheless, Runs 1–3 yielded assignments of virtually equal correctness (Table 2). Runs 4 and 5 were of reduced quality, but still generated the proper structure. However, in Run 6 there is an obvious deterioration in the backbone fold.

The backbone and βCH_n assignments are the most accurate, with 96–97% of these shifts being equal to the reference assignments for Runs 1–3, 92–93% for Runs 4 and 5, and 88% for Run 6. Two percent of the backbone and βCH_n shifts in Runs 1–3, 3–6% in Runs 4–5, and 12% in Run 6 are not assigned to the correct residue. The accuracy of the

side-chain assignments beyond βCH_n is lower, with 5–6% of the shifts in Runs 1–3, 10–11% in Runs 4–5, and 19% in Run 6 not being assigned to the correct residue. Overall, the assignments to incorrect residues amount to 3–4% for Runs 1–3, 6–7% for Runs 4–5, and 15% for Run 6. With the exception of Run 6, this extent of errors fulfills the previously established minimal requirement of 90% assignment for the successful use of combined automated NOE assignment and structure calculation with CYANA.^{6,20}

The consensus chemical shift assignments were used together with the automatically picked NOESY peak lists for the assignment of NOEs and the structure calculation. The total number of input NOESY cross peaks was 13 894. This number is considerably larger than the total number of 7012 expected NOESY cross peaks, 1340 in the ^{15}N -edited NOESY spectrum and 5672 in the ^{13}C -edited NOESY spectrum, based on a maximal observable ^1H – ^1H distance of 4.5 Å in the reference structure 1WQU. In comparison, the manually prepared NOESY peak lists for the conventional structure determination contained 4732 NOESY peaks, of which 4603 were assigned.⁸ The number of NOESY peaks assigned using the FLYA method varied from 4882 in Run 1

to 4524 in Run 6 (Table 2). Among the distance restraints derived from the assigned NOEs there were 1206–1230 long-range distance restraints for Runs 1–3, 1153–1188 for Runs 4–5, and 1102 for Run 6. The resulting structures are visualized in Fig. 2. The final CYANA target function values do not vary significantly over Runs 1–4 (values of 3.2–4.7 Å²), and increase moderately to 7.6–8.8 Å² for Runs 5–6. The same holds true for the maximal residual restraint violations, which do not exceed 0.2 Å in Runs 1–6 but are higher for Runs 5–6, and the conformational energies that are roughly 200 kcal/mol less favorable for Runs 5–6 than for the other runs. The precision of the structure bundles, as measured by the RMSD to their mean coordinates for the structured region, is essentially the same for all runs (Table 2). These RMSD values vary in the narrow ranges of 0.30–0.35 Å for the backbone, and 0.68–0.74 Å for all the heavy atoms. This underlines the earlier finding²⁰ that the precision of a structure bundle is not a suitable indicator of its accuracy, in particular, when using automated NOESY assignment.

The accuracy of the structures was assessed quantitatively by comparison with the 1WQU reference structure⁸ that was determined previously by conventional methods. The RMSD values to the reference structure varied for Runs 1–4 in the range of 0.85–1.06 Å for the backbone and 1.33–1.56 Å for all the heavy atoms. Slightly higher values of 1.28/1.83 Å were obtained in Run 5. It is only when a single backbone experiment and no side-chain experiments are used in Run 6 that the backbone fold begins to break down, as evidenced by RMSD values to the reference structure of 2.87 and 3.41 Å for the backbone and all the heavy atoms, respectively. Run 6, with 15% of all nuclei not being assigned to the correct residue (Table 2), did not fulfill the requirement of 90% correct chemical shift assignments for a successfully automated NOE assignment with CYANA.^{6,20} In Run 6, there was not enough information for the algorithm to properly assign the backbone and side-chain atoms, thus leading to a loss of structure. Nevertheless, the global fold obtained in Run 6 is still clearly similar to that of the reference structure.

The close similarity of the results from Runs 1–3 indicates that for Fes SH2 all the essential information for the assignment of the polypeptide backbone could be obtained

from the two spectra, CBCA(CO)NH and CBCANH, and that the HCCH-COSY spectrum was not crucial for the assignment of side-chain chemical shifts, provided that the other four side-chain assignment spectra were available. Additionally, omitting the HCCH-TOCSY spectrum led to a marked increase of the chemical shift assignment errors in Run 4, but only to a marginal decrease of the structural quality. Run 5 used only a single backbone experiment, CBCA(CO)NH, and two side-chain experiments, (H)CC(CO)NH and H(CCCO)NH. The extent of incorrect backbone chemical shift assignments is increased and the accuracy of the structure significantly decreased in Run 5 compared to Run 4.

The FLYA method provides chemical shift assignments for all atoms that are assigned to at least one peak in any of the input spectra, including the atoms in the unstructured regions, most of which were not assigned during the conventional determination.⁹ Many of the chemical shift assignments by FLYA for the unstructured regions must therefore be considered as unreliable. Questionable NOE assignments involving such unreliably assigned chemical shifts and, for example, artifact peaks, may result in the appearance of well-defined structures for parts of the protein that are actually unstructured in solution. In the case of Fes SH2 the only unstructured regions are the N- and C-termini. Such artifactually ordered structures were observed in stage I of some of the FLYA calculations. However, for Runs 1–5, both tails were disordered in the final structures obtained at the end of stage III. Only in Run 6, in which the backbone fold was partially flawed, was the C-terminal tail structured in two of the three FLYA calculations. This indicates that network anchoring⁶ was effective in eliminating the spurious NOE assignments that do not form part of the self-consistent network of correctly assigned NOEs. Caution should be applied when using the FLYA method with data sets of severely limited information content since it is possible that flexible regions will be improperly ordered. However, such problems can usually be detected readily by analyzing the quality parameter for the consensus chemical shifts that are calculated by the FLYA algorithm. For instance, in Runs 1–5 less than 50% of the chemical shifts in the tail regions of residues 1–7 and 109–114 were classified as reliable consensus assignments, whereas the corresponding percentage was always above 80 for the structured region of residues 8–108. The conformation of stretches of the polypeptide chain with many unreliable chemical shift assignments must be considered as unreliable.

CONCLUSIONS

The results of this case study for the Fes SH2 protein indicate that fully automated NMR protein structure determination is possible using seven to eight 3D NMR experiments, including two NOESY, two backbone, and three to four side-chain experiments. In a future study we plan to investigate what happens when the information content of individual data sets is less complete because of either lower protein concentrations or broader linewidths in parts or all of the protein. The present results suggest that slightly lower data

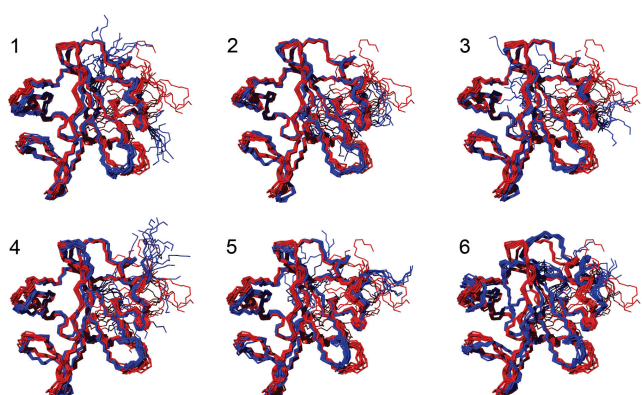


Figure 2. Fes SH2 domain structures from FLYA runs 1–6 (red) superimposed on the conventionally determined solution structure⁸ (blue).

quality for individual spectra may be tolerable provided that there is sufficient redundancy within the full set of spectra. Ideally, an approach that is based exclusively on spectra that yield conformational restraints, i.e. the NOESY experiments, is the most attractive. However, with the present version of FLYA a few through-bond experiments remain necessary for reliable results. It will be intriguing to combine the FLYA approach with optimal isotope labeling by the SAIL (stereo-array isotope labeling) method^{21,22} to enhance the efficiency, reliability, and size range of applicability of fully automated NMR protein structure determination. In this way, a further reduction in the required number of experiments is conceivable without the loss of crucial information because SAIL gives rise to fewer and sharper peaks, reduces the number of signals to be assigned, and eliminates the need for stereospecific assignments.

Acknowledgements

A.S. was supported by the Japan Society for the Promotion of Science. This work was supported by the National Project on Protein Structural and Functional Analyses of the Ministry of Education, Culture, Sports, Science and Technology of Japan (MEXT), and by the Tatsuo Miyazawa Memorial Program of RIKEN Genomic Sciences Center.

REFERENCES

1. Baran MC, Huang YJ, Moseley HNB, Montelione GT. *Chem. Rev.* 2004; **104**: 3541.
2. Altieri AS, Byrd RA. *Curr. Opin. Struct. Biol.* 2004; **14**: 547.
3. Gronwald W, Kalbitzer HR. *Prog. NMR Spectrosc.* 2004; **44**: 33.
4. Güntert P. *Prog. NMR Spectrosc.* 2003; **43**: 105.
5. Nilges M, Macias MJ, O'Donoghue SI, Oschkinat H. *J. Mol. Biol.* 1997; **269**: 408.
6. Herrmann T, Güntert P, Wüthrich K. *J. Mol. Biol.* 2002; **319**: 209.
7. Huang YJ, Moseley HNB, Baran MC, Arrowsmith C, Powers R, Tejero R, Szyperski T, Montelione GT. *Methods Enzymol.* 2005; **394**: 111.
8. Scott A, Pantoja-Uceda D, Koshiba S, Inoue M, Kigawa T, Terada T, Shirouzu M, Tanaka A, Sugano S, Yokoyama S, Güntert P. *J. Biomol. NMR* 2005; **31**: 357.
9. Scott A, Pantoja-Uceda D, Koshiba S, Inoue M, Kigawa T, Terada T, Shirouzu M, Tanaka A, Sugano S, Yokoyama S, Güntert P. *J. Biomol. NMR* 2004; **30**: 463.
10. Johnson BA, Blevins RA. *J. Biomol. NMR* 1994; **4**: 603.
11. Güntert P, Mumenthaler C, Wüthrich K. *J. Mol. Biol.* 1997; **273**: 283.
12. Bartels C, Güntert P, Billeter M, Wüthrich K. *J. Comput. Chem.* 1997; **18**: 139.
13. Bartels C, Billeter M, Güntert P, Wüthrich K. *J. Biomol. NMR* 1996; **7**: 207.
14. Malmodin D, Papavoine CHM, Billeter M. *J. Biomol. NMR* 2003; **27**: 69.
15. Cornell WD, Cieplak P, Bayly CI, Gould IR, Merz KM, Ferguson DM, Spellmeyer DC, Fox T, Caldwell JW, Kollman PA. *J. Am. Chem. Soc.* 1995; **117**: 5179.
16. Koradi R, Billeter M, Güntert P. *Comput. Phys. Commun.* 2000; **124**: 139.
17. Luginbühl P, Güntert P, Billeter M, Wüthrich K. *J. Biomol. NMR* 1996; **8**: 136.
18. Delaglio F, Grzesiek S, Vuister GW, Zhu G, Pfeifer J, Bax A. *J. Biomol. NMR* 1995; **6**: 277.
19. Koradi R, Billeter M, Wüthrich K. *J. Mol. Graphics* 1996; **14**: 51.
20. Jee J, Güntert P. *J. Struct. Funct. Genomics* 2003; **4**: 179.
21. Kainosho M, Torizawa T, Iwashita Y, Terauchi T, Ono AM, Güntert P. *Nature* 2006; **439**: 52.
22. Ikeya T, Terauchi T, Güntert P, Kainosho M. *Magn. Reson. Chem.* 2006; **44**: S152.